

## Abstract

We report a new approach for modeling reversible self- and hetero-associations with sedimentation velocity (SV) experiments. The approach allows us to measure dissociation constants and also to derive kinetic rate constants by modeling perturbations observed only in SV when kinetics of associations are slower than the sedimentation rate of the solutes involved in the reaction. New finite element models were developed and implemented in UltraScan to describe mass action processes occurring during SV experiments, and are used here to fit experimental data and obtain kinetic rate constants and dissociation constants. The method is capable of characterizing small amounts of impurities and provides a more reliable measurement of equilibrium constants than is possible with sedimentation equilibrium (SE) experiments. Example systems are presented to illustrate this new capability.

## Introduction

Analytical ultracentrifugation has long been accepted as the gold standard for the characterization of macromolecular properties as well as the properties of reversible and irreversible reactions among macromolecules in the solution phase. Two principle experiments are generally performed in the analytical ultracentrifuge, SV and SE. SV experiments are performed at higher speed, and observe the macromolecular sedimentation and diffusion transport by monitoring the concentration profiles of all solutes present in the solution over time. SE experiments monitor the equilibrium gradients obtained at the end of the SV experiment when all flow ceases and sedimentation and diffusion transport are exactly balanced. In SE experiments, the distribution of all reacting species obeys mass-action laws at equilibrium, however, in SV experiments the equilibration due to mass action can be perturbed in a predictable manner if the sedimentation rate exceeds the rate constant of the reaction (see Fig. 1).

### Monomer – Trimer Equilibrium, Monomer MW = 50 kDa

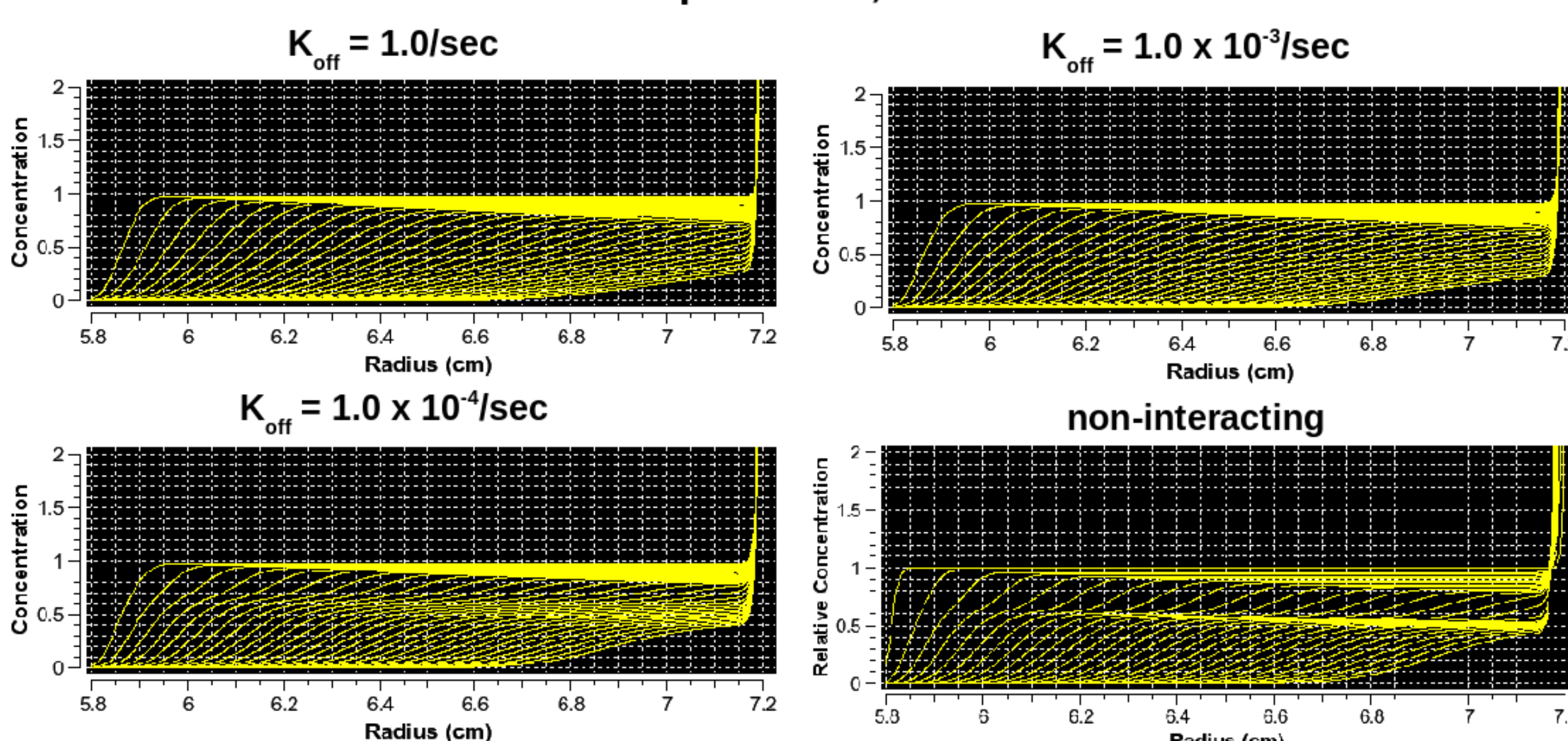


Figure 1: Kinetic effect on the sedimenting boundary.

The observed perturbation is a function of the rotor speed and the difference of the sedimentation coefficients of the reacting solutes, which is a function of their mass and shape. In rapidly equilibrating SV experiments the thermodynamic equilibration speed exceeds the sedimentation speed, and apparent hydrodynamic species at each point in the concentration gradient are represented by the weight-average sedimentation coefficient and the gradient-average diffusion coefficient of all reacting species [TH81] (see Eq. 1):

$$\bar{s} = \frac{\sum_{j=1}^m s_j C_j}{C_T} = \frac{\sum_{j=1}^m s_j K_j C_1^j}{C_T} \quad \bar{D} = \frac{\sum_{j=1}^m D_j (\partial C_j / \partial r)}{\sum_{j=1}^m (\partial C_j / \partial r)} = \frac{\sum_{j=1}^m j D_j K_j C_1^{j-1}}{\sum_{j=1}^m j K_j C_1^{j-1}}$$

Equation 1: Formula for weight-average sedimentation coefficient and gradient-average diffusion coefficient ( $m$ =number of reacting species).

When the reaction rate is slow compared to the sedimentation rate, the reacting species are separated before being able to re-equilibrate, and discrete species will be observed similar to what is observed in a non-interacting system [C78].

## Identifying a Reversible System with van Holde - Weischet

A reversibly associating system with finite reaction kinetics will not produce discrete species, but rather a continuous *reaction boundary* of species representing the weight average of the constituent species. The relative amount of each species depends on the loading concentration and equilibrium constant of the system. Hence, a reacting system can be clearly distinguished from a non-interacting system by two analysis results that are readily observed in a van Holde - Weischet integral distribution plot: 1. The shape of the integral distribution (indicating the reaction rate) and the position of the integral distribution (indicating the  $K_d$ ). This is shown in Figs. 2 and 3.

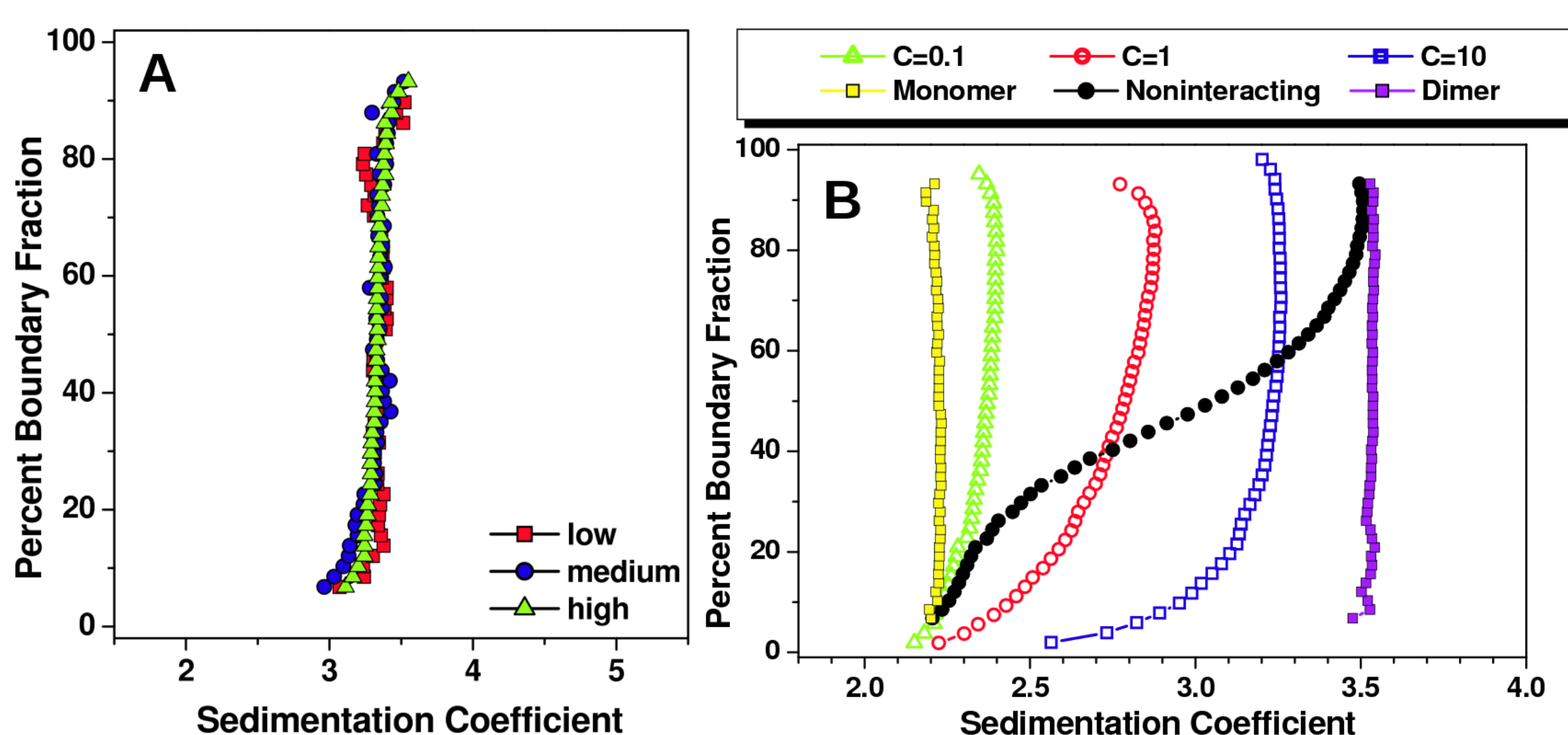


Figure 2: van Holde – Weischet integral distribution plots for 3 concentrations of ovalbumin (A) and a rapidly reversible self-associating monomer dimer system (B). The black line indicates the sedimentation distribution for a non-interacting system with the same hydrodynamic properties as the monomer and dimer.

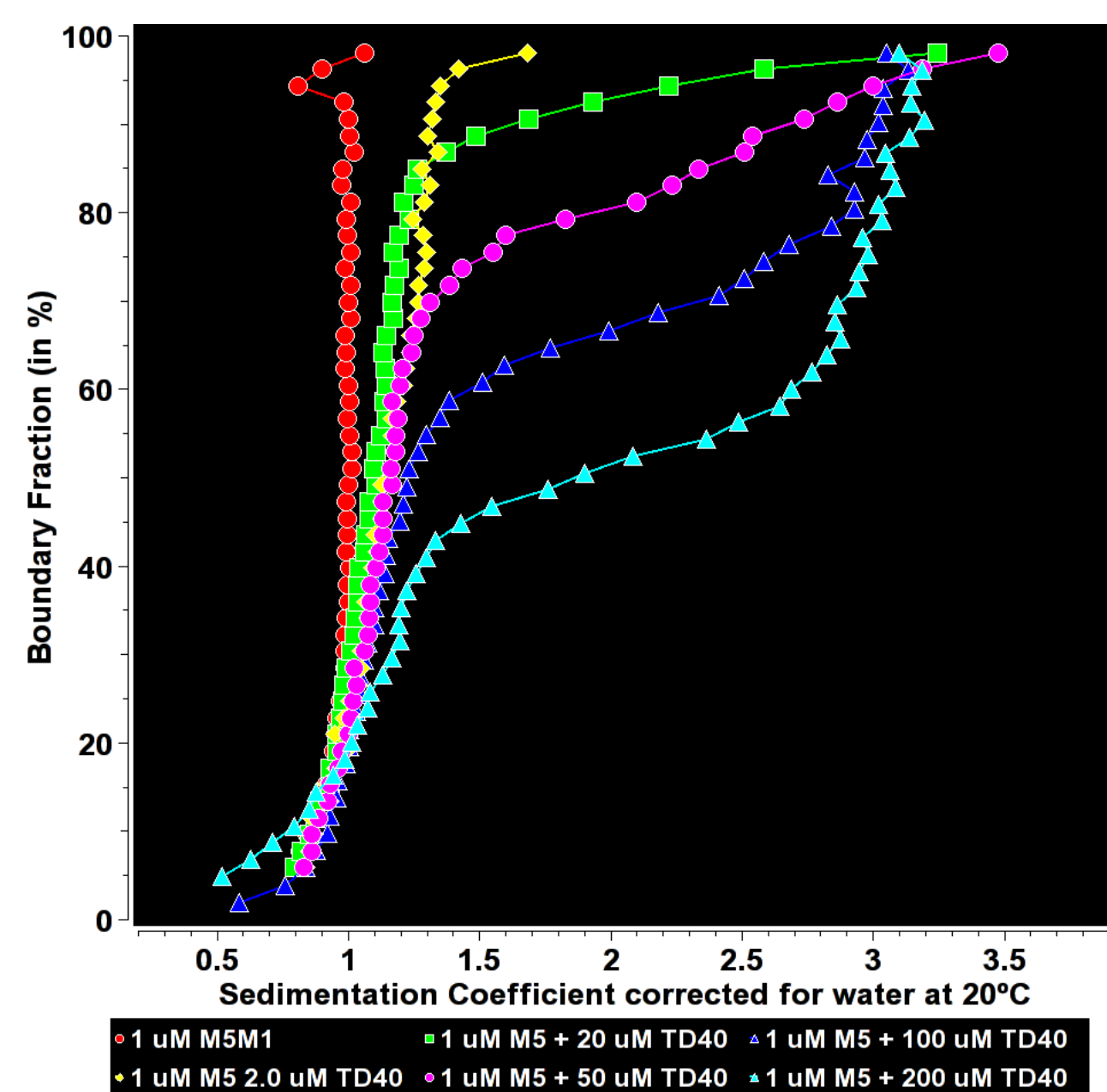


Figure 3: van Holde – Weischet integral distribution plots for a titration of 1-200  $\mu$ M clathrin TD40 against a 1  $\mu$ M Alexa-488 labeled peptide, M5M1, a fragment of the AP180 clathrin assembly protein with a single clathrin binding site. The data indicate a slow kinetic rate constant and a binding  $K_d$  of approximately 200  $\mu$ M. The TD40 protein is not visible by itself because it is not labeled, only the free M5M1 peptide and its complex with TD40 is visible. The complex sediments at approximately 3.5 s, M5M1 has a sedimentation rate of 1s.

## Kinetic Rate Constant Signal

The relative signal available for modeling can be measured as a function of the residual mean square deviation (RMSD) between a system with a finite reaction rate and one with an infinitely fast reacting rate constant. The larger the RMSD, the larger the signal available for fitting, and the higher the confidence in the determined parameter. Fig. 4 shows the RMSD for a monomer dimer reaction measured at 60 krpm for four different molecular weight species, all simulated with a frictional ratio of 1.25, corresponding to a globular protein.

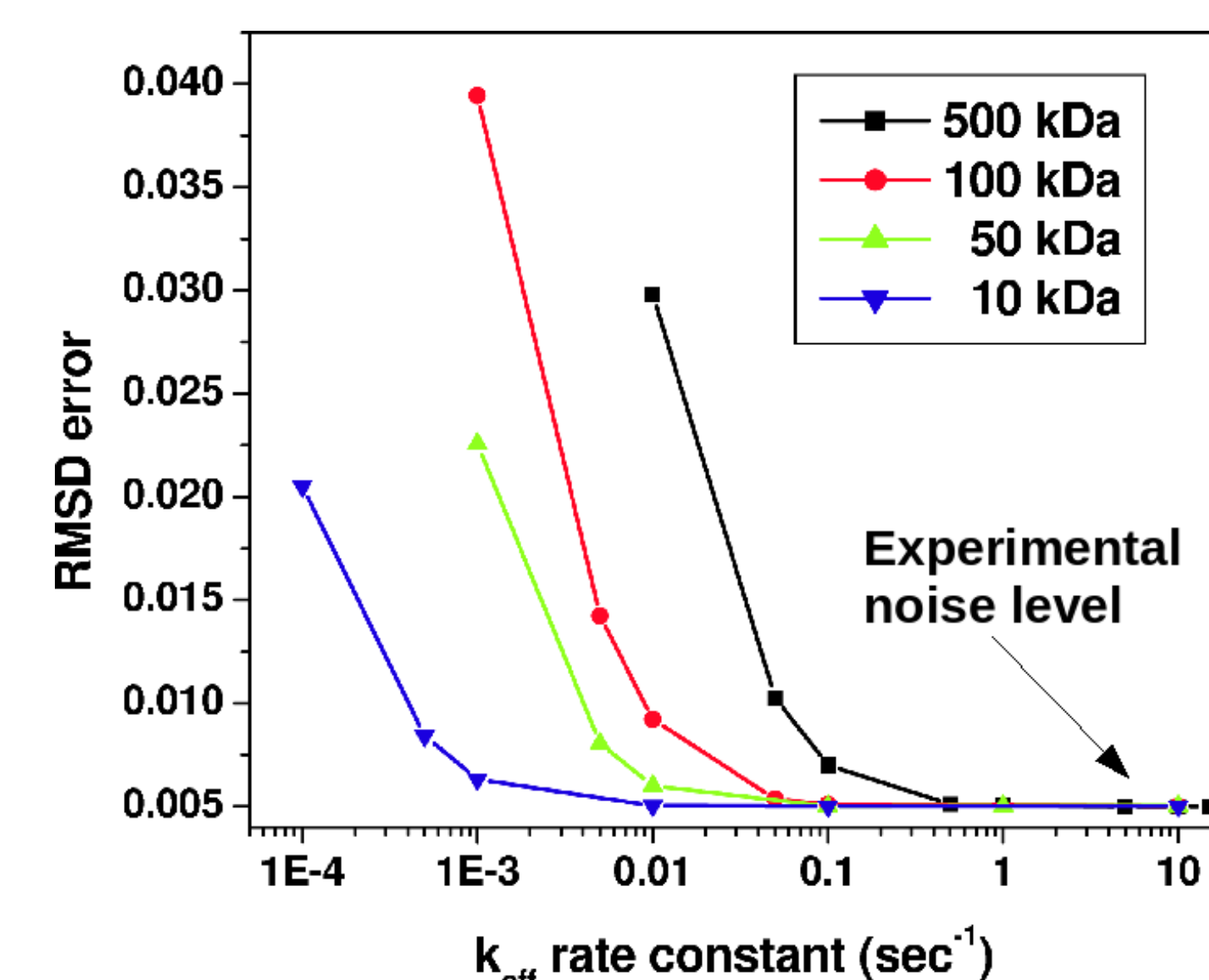


Figure 4: RMSD comparison between infinitely fast reacting associations and finite reaction rates for a series of molecular weights at 60 krpm. The larger the molecular weight, the greater is the kinetic effect on the boundary shape. A higher RMSD translates to a higher confidence in the determination of the rate constant.

For the determination of the rate constant, the sample should be measured at the fastest speed possible with the ultracentrifuge to maximize the kinetic signal.

## Whole Boundary Modeling Approach

The flow of the sedimenting solutes in the analytical ultracentrifuge cell is governed by the Lamm equation [L29] (Eq. 2), subject to the kinetic effect and the constraints shown in Eq. 1.

$$L(s, D): \left( \frac{\partial C}{\partial t} \right)_r = \frac{-1}{r} \frac{\partial}{\partial r} \left[ s \omega^2 r^2 C - D r \frac{\partial C}{\partial r} \right],$$

Equation 2: Lamm equation for the flow of a solute in a sector-shaped cell

The Lamm equation for the reacting case can be solved with an adaptive space-time finite element solution [CD08]. The inverse problem of fitting experimental data to the finite element solution is accomplished with the genetic algorithm [BD07], a stochastic optimization approach that improves the fitting parameters using evolutionary paradigms and random operators (see Fig 5).

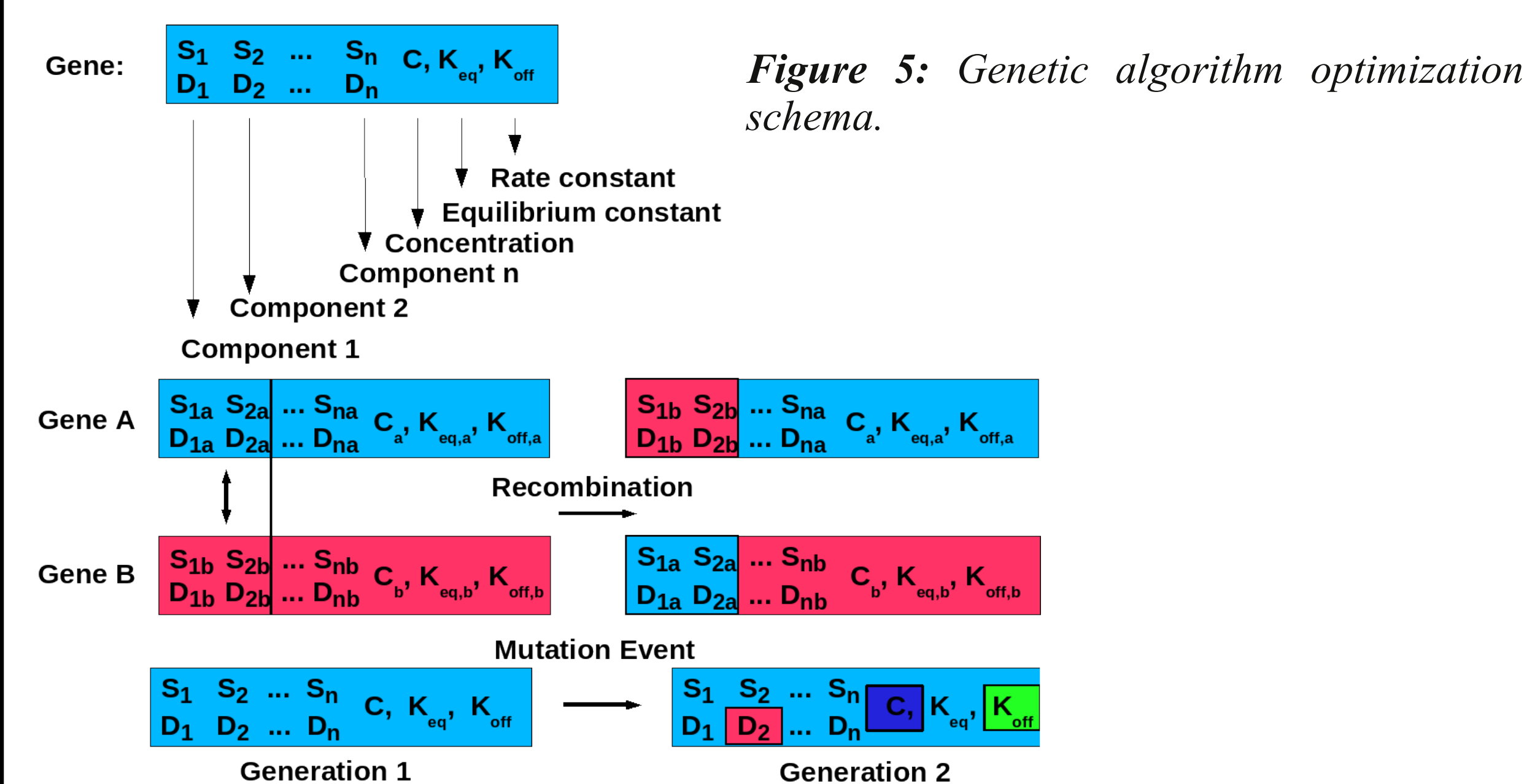


Figure 5: Genetic algorithm optimization schema.

## Experimental Results:

Our first dataset demonstrates the reproducibility of our approach by analyzing a simulated monomer-dimer dataset with realistic noise added. With such simulated data the performance of the optimization method can be ascertained, and the fitting results can be directly compared to the input parameters (Table 1). Secondly, we compared the SV results of the C-terminal domain of the human Polycomb Group protein RING1B (C-RING1B) for wildtype and the K261A mutant (Table 2). C-RING1B dimerizes weakly in solution with a  $K_d$  in a suitable concentration range [DK10].

Parameter	Fitted value	95% confidence interval	Target value	% A
Monomer s value:	2.215e-13 s	(2.166e-13, 2.263e-13)	2.214e-13 s	0.05
Monomer D value:	9.596e-07 cm <sup>2</sup> /s	(8.857e-07, 1.033e-06)	9.595e-07 cm <sup>2</sup> /s	0.01
Monomer MW	1.996e+04 Da	(1.863e+04, 2.129e+04)	2.000e+04 Da	0.20
Monomer f/f <sub>0</sub> :	1.250E+00	(1.179e+00, 1.321e+00)	1.250E+00	0.00
Dimer s value:	3.578e-13 s	(3.461e-13, 3.696e-13)	3.515e-13 s	1.79
Dimer D value:	7.754e-07 cm <sup>2</sup> /s	(7.363e-07, 8.144e-07)	7.616e-07 cm <sup>2</sup> /s	1.81
Dimer mol. weight:	3.992e+04 Da	(3.725e+04, 4.259e+04)	4.000e+04 Da	0.20
Dimer f/f <sub>0</sub> :	1.221E+00	(1.190e+00, 1.252e+00)	1.250E+00	2.37
K <sub>d</sub>	9.055E-01	(6.962e-01, 1.115e+00)	1.000E+00	10.44
k <sub>on</sub> rate constant:	1.466e-03 s <sup>-1</sup>	(8.591e-04, 2.0723e-03)	1.000e-03 s <sup>-1</sup>	46.60

Table 1: Genetic algorithm fitting results for a 20 kDa simulated monomer-dimer system containing 0.5% noise. All parameters were floated. All target parameter values were reproduced by the fit within the 95% confidence intervals.

Parameter:	wildtype, 0.9 OD	K261A, 0.9 OD
Sed. veloc. K <sub>s</sub> ( $\mu$ M)	17.6 (14.8, 21.6)	28.5 (25.8, 31.8)
Sed. equil. K <sub>s</sub> ( $\mu$ M)	22.7 (8.64, 63.0)	54.0 (29.1, 166.1)
k <sub>on</sub> ( $\times 10^3$ sec <sup>-1</sup> )	84.3 (48.6, 120.0)	14.1 (8.1, 20.1)
f/f <sub>0</sub> (monomer)	1.14 (1.09, 1.19)	1.19 (1.17, 1.21)
f/f <sub>0</sub> (dimer)	1.31 (1.30, 1.32)	1.44 (1.43, 1.45)
f/f <sub>0</sub> (contaminant)	1.24 (1.18, 1.3)	1.49 (1.47, 1.56)
contam. OD (x0.01)	3.56 (3.37, 3.75)	2.77 (2.58, 2.96)
mol. wt. (x1000)	2.33 (2.09, 2.56)	3.00 (2.93, 3.06)

Table 2: SV fitting results for C-RING1B wildtype and K261A mutant to a reversible monomer dimer equilibrium model that allows for the presence of a contaminant. Values in parentheses represent 95% confidence intervals.

## References

- [TH81] Todd, G. P., and R. H. Haschemeyer. General solution to the inverse problem of the differential equation of the ultracentrifuge. *Proc. Natl. Acad. Sci. USA.* **1981**, 78 11:6739-6743.
- [C78] Cann JR. Kinetically controlled mass transport of associating-dissociating macromolecules. *Methods Enzymol.* **1978**, 48 248-270.
- [L29] Lamm, O. Die Differentialgleichung der Ultracentrifugierung. *Ark. Mat. Astron. Fys.* **21B** (1929) 1-4.
- [CD08]Cao, W and B. Demeler. Modeling Analytical Ultracentrifugation Experiments with an Adaptive Space-Time Finite Element Solution for Multi-Component Reacting Systems. *Biophys. J.* **2008**, 95(1):54-65
- [BD07] Brookes, E and B. Demeler. Parsimonious Regularization using Genetic Algorithms Applied to the Analysis of Analytical Ultracentrifugation Experiments. *GECCO Proceedings, 2007*, ACM 978-1-59593-697-4/07/0007
- [DK10]Demeler B, Brookes E, Wang R, Schirf V, Kim CA. Characterization of Reversible Associations by Sedimentation Velocity with UltraScan. *Macromol. Biosci.* (2010), in press

**Abstract**  
We report a new approach for modeling reversible self- and hetero-associations with sedimentation velocity (SV) experiments. The approach allows us to measure dissociation constants and also to derive kinetic rate constants by modeling perturbations observed only in SV when kinetics of association is slower than the sedimentation rate of the solutes involved in the reaction. New finite element codes were developed and implemented in UltraScan to describe mass action processes occurring during SV experiments, and are used here to fit experimental data and obtain kinetic rate constants and association constants. The method is capable of characterizing initial amounts of impurities and provides a more reliable measurement of equilibrium constants than is possible with sedimentation equilibrium (SE) experiments. Example systems are presented to illustrate this new capability.

**Introduction**  
Analytical ultracentrifugation has long been accepted as the gold standard for the characterization of macromolecular properties as well as the properties of reversible and irreversible reactions among macromolecules in the solution phase. Two principle experiments are generally performed in the analytical ultracentrifuge, SV and SE. SV experiments are performed at higher speed, and observe the macromolecular sedimentation and diffusion transport by monitoring the concentration profiles of all solutes present in the solution over time. SE experiments monitor the equilibrium gradients obtained at the end of the SV experiment when all flow ceased and sedimentation and diffusion transport are exactly balanced. In SE experiments, the distribution of all reacting species obeys mass-action laws at equilibrium, however, in SV experiments the equilibrium due to mass action can be perturbed in a predictable manner if the sedimentation rate exceeds the rate constant of the reaction (see Fig. 1).

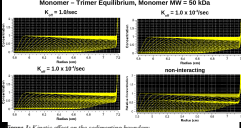


Figure 1: Kinetic effect on the sedimenting boundary.

The observed perturbation is a function of the rotor speed and the difference of the sedimentation coefficients of the reacting species, which is a function of their mass and shape. In rapidly equilibrating SV experiments the thermodynamic equilibrium speed exceeds the sedimentation speed, and apparent hydrodynamic species at each point in the concentration gradient are represented by the weight-average sedimentation coefficient and the gradient-average diffusion coefficient of all reacting species [TH81] (see Eq. 1):

$$s_{app} = \frac{\sum_i s_i C_i}{\sum_i C_i} \quad D = \frac{\sum_i D_i C_i}{\sum_i C_i}$$

Equation 1: Formula for weight-average sedimentation coefficient and gradient average diffusion coefficient (in number of reacting species).

When the reaction rate is slow compared to the sedimentation rate, the reacting species are separated before being able to re-equilibrate, and discrete species will be observed similar to that observed in a non-interacting system [C79].

**Modeling a reversibly associating system with finite reaction kinetics**  
A reversibly associating system with finite reaction kinetics will not produce discrete species, but rather a continuous reaction boundary of species representing the weight average of the constituent species. The relative amount of each species depends on the loading concentration and equilibrium constants of the system. Hence, a reacting system can be clearly distinguished from a non-interacting system by two analytical results that are readily observed in a van Holde - Weisbach integral distribution plot: 1. The shape of the integral distribution (indicating the reaction rate) and the position of the integral distribution (indicating the KD). This is shown in Figs. 2 and 3.

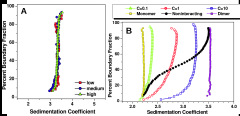


Figure 2: van Holde - Weisbach integral distribution plots for 3 concentrations (100 nM, 50 nM, and 10 nM) of a reversibly associating monomer-dimer system. The black line indicates the sedimentation distribution for a non-interacting system. The curves show the effect of reaction kinetics on the sedimentation distribution.

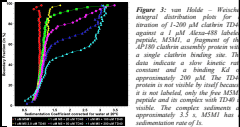


Figure 3: van Holde - Weisbach integral distribution plots for a reaction of 1:200. The curves show the effect of reaction kinetics on the sedimentation distribution.

**Kinetic Rate Constant Signal**  
The relative signal available for modeling can be measured as a function of the residual mean square deviation (RMSD) between a system with a finite reaction rate and one with an infinitely fast reaction rate. The larger the RMSD, the larger the signal available for fitting, and the higher the confidence in the determined parameter. Fig. 4 shows the RMSD for a monomer-dimer reaction measured at 60 kpm for four different molecular weight species, all simulated with a rotational ratio of 1.25, corresponding to a globular protein.

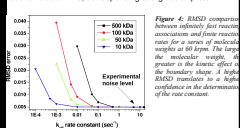


Figure 4: RMSD comparison between infinitely fast reaction and finite reaction rates. The plot shows RMSD vs. 'K on concentration' for four different molecular weight species.

**Whole boundary modeling Approach**  
The flow of the sedimenting solutes in the analytical ultracentrifuge cell is governed by the Lamm equation (Eq. 2), subject to the kinetic effect and the constants shown in Eq. 1:

$$L(r, D) \left( \frac{\partial C}{\partial t} + \frac{\partial}{\partial r} \left[ s \omega^2 r C - D r \frac{\partial C}{\partial r} \right] \right) = 0$$

Equation 2: Lamm equation for the flow of a solute in a rotor-shaped cell. The Lamm equation for the reacting case can be solved with an adaptive space-time finite element solution [C08]. The inverse problem of fitting experimental data to the finite element solution is accomplished with the genetic algorithm [B07], a stochastic optimization approach that improves the fitting parameters using evolutionary paradigms and random operators (see Fig 5).

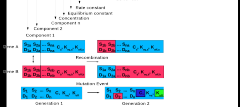


Figure 5: Genetic algorithm optimization scheme.

**Experimental Results:**  
Our first dataset demonstrates the reproducibility of our approach by analyzing a simulated monomer-dimer dataset with realistic noise added. With such simulated data the performance of the optimization method can be ascertained and the fitting results can be directly compared to the input parameters (Table 1). Secondly, we compared the SV results of the C-terminal domain of the human Polycomb Group protein RING1B (C-RING1B) for wildtype and the K261A mutant (Table 1). C-RING1B dimerizes weakly in solution with a KD in a suitable concentration range [DK10].

Parameter	Input	Output
$K_D$ [nM]	100	100
$k_{on}$ [1/s]	1000	1000
$k_{off}$ [1/s]	10000	10000
$s_M$ [S]	10000	10000
$s_D$ [S]	20000	20000
$D_M$ [cm <sup>2</sup> /s]	100000	100000
$D_D$ [cm <sup>2</sup> /s]	200000	200000

Parameter	Wildtype	K261A
$K_D$ [nM]	100	100
$k_{on}$ [1/s]	1000	1000
$k_{off}$ [1/s]	10000	10000
$s_M$ [S]	10000	10000
$s_D$ [S]	20000	20000
$D_M$ [cm <sup>2</sup> /s]	100000	100000
$D_D$ [cm <sup>2</sup> /s]	200000	200000

**References**  
[TH81] Todd, G. P., and R. H. Trewhella. General solution to the inverse problem of the ultracentrifuge. *Proc. Natl. Acad. Sci. USA*, 78, 11, 6333-6337, 1981.  
[C79] Cass, J.B. Kinetically controlled mass transport of interacting-dissociating macromolecules. *Methods Enzymol.* 79B, 49-109, 1981.  
[C08] Lafer, E. and B. Demeler. Inverse Element Solution for Multi-Component Reacting Systems. *J. Math. Biol.* 56(1), 5-45, 2008.  
[B07] Brookes, E. and B. Demeler. Stochastic Optimization using Genetic Algorithms applied to the Analysis of Analytical Ultracentrifugation Experiments. *CECCO Proceedings*, 2007. <http://www.utsa.edu/~demeler/CECCO07/>  
[DK10] Demeler, B., Brookes, E., Wang, R., Schif, V., Kim, C.A. Characterization of Reversible Association by Sedimentation Velocity with UltraScan. *Biophysical Journal* 98(10), 2009.